
Advancing Multimodal Reasoning Capabilities of Multimodal Large Language Models via Visual Perception Reward

Tong Xiao¹, Xin Xu⁴, Zhenya Huang^{1,2}, Hongyu Gao³, Quan Liu^{2,3},
 Qi Liu^{1,2}, Enhong Chen^{1,2*}

¹University of Science and Technology of China

²State Key Laboratory of Cognitive Intelligence

³iFLYTEK AI Research

⁴Hong Kong University of Science and Technology

Abstract

Enhancing the multimodal reasoning capabilities of Multimodal Large Language Models (MLLMs) is a challenging task that has attracted increasing attention in the community. Recently, several studies have applied Reinforcement Learning with Verifiable Rewards (RLVR) to the multimodal domain in order to enhance the reasoning abilities of MLLMs. However, these works largely overlook the enhancement of multimodal perception capabilities in MLLMs, which serve as a core prerequisite and foundational component of complex multimodal reasoning. Through McNemar’s test, we find that existing RLVR method fails to effectively enhance the multimodal perception capabilities of MLLMs, thereby limiting their further improvement in multimodal reasoning. To address this limitation, we propose Perception-R1, which introduces a novel visual perception reward that explicitly encourages MLLMs to perceive the visual content accurately, thereby can effectively incentivizing both their multimodal perception and reasoning capabilities. Specifically, we first collect textual visual annotations from the CoT trajectories of multimodal problems, which will serve as visual references for reward assignment. During RLVR training, we employ a judging LLM to assess the consistency between the visual annotations and the responses generated by MLLM, and assign the visual perception reward based on these consistency judgments. Extensive experiments on several multimodal reasoning benchmarks demonstrate the effectiveness of our Perception-R1, which achieves state-of-the-art performance on most benchmarks using only 1,442 training data. Our code and dataset will be available at <https://github.com/tongxiao2002/Perception-R1>.

1 Introduction

Multimodal reasoning is a fundamental capability for AI systems to solve complex real-world tasks and represents a critical step toward artificial general intelligence (AGI). Since the emergence of Multimodal Large Language Models (MLLMs), extensive studies have been proposed to enhance their multimodal reasoning capabilities. Early efforts focused on prompt engineering techniques [62, 63, 57, 36], while subsequent works leveraged supervised fine-tuning (SFT) with high-quality reasoning datasets [16, 43, 38, 61]. More recently, the success of reasoning models such as OpenAI-o1 [21], DeepSeek-R1 [17], and Kimi-k1.5 [45] has demonstrated the efficacy of large-scale reinforcement

*Corresponding author.

 <p>Question: Chords \overline{AC} and \overline{DF} are equidistant from the center. If the radius of $\odot G$ is 26, find DE.</p> <p>Answer: 24</p>	<p>Qwen2.5-VL-7B-IT</p> <p>To solve for the length of DE, we need to use the properties of circles and the given information.</p> <p>1. Identify the given information:</p> <ul style="list-style-type: none"> The radius of $\odot G$ is 26. <p>.....</p> <p>2. Determine the perpendicular distances:</p> <ul style="list-style-type: none"> The distance from the center G to \overline{AC} is 10. The distance from the center G to \overline{DF} is 10. <p>3. Use the Pythagorean theorem in the right triangles formed:</p> <ul style="list-style-type: none"> Consider the right triangle $\triangle OAE$ (where O is the midpoint of \overline{AC} and E is the midpoint of \overline{DF}). The radius OA is 26 and the perpendicular distance from G to \overline{AC} is 10. <p>4. Calculate the length of AE:</p> $AE = \sqrt{OA^2 - OG^2} = \sqrt{26^2 - 10^2} = 24$ <p>5. Determine the length of DE:</p> <ul style="list-style-type: none"> Since E is the midpoint of \overline{DF}, the length of DE is the same as the length of AE because \overline{AC} and \overline{DF} are equidistant from the center and thus symmetric in the circle. <p>Therefore, the length of DE is 24.</p> <p>Qwen2.5-VL-7B-IT Trained by RLVR</p> <p><think></p> <p>To find the length of DE, we need to use the property that chords equidistant from the center of a circle are congruent. This means that $AC = DF$. Given:</p> <ul style="list-style-type: none"> The radius $RG = 26$ The distance from the center G to chord \overline{AC} is the same as the distance from the center G to chord \overline{DF}, which is 10. <p>For chord \overline{AC}, the perpendicular from G to \overline{AC} creates two right triangles, $\triangle AGB$ and $\triangle AGB$, which are congruent. The same applies to chord \overline{DF} with $\triangle DGE$ and $\triangle DGE$. The length of half of chord \overline{AC} can be found using the Pythagorean theorem in $\triangle AGB$:</p> $AG = \sqrt{RG^2 - GB^2} = \sqrt{26^2 - 10^2} = 24.$ <p>Since AC and DF are equidistant and congruent in length, $DF = 48$. Applying the same logic to chord \overline{DF}, we use the right triangle $\triangle DGE$:</p> $DG = \sqrt{RG^2 - GE^2} = \sqrt{26^2 - 10^2} = 24.$ <p>So, $DF = 2 \times DE$. Since $DF = 48$, we have:</p> $DE = \frac{DF}{2} = \frac{48}{2} = 24$ <p></think></p> <p>Perception-R1</p> <p><think></p> <p>Looking at the image, we can see that \overline{AC} and \overline{DF} are equidistant from the center G, which means the perpendicular distances from G to \overline{AC} and \overline{DF} are the same. This implies that the perpendiculars from G to \overline{AC} and \overline{DF} will intersect \overline{AC} and \overline{DF} at their midpoints, say B and E respectively, because the chords are equidistant from the center.</p> <p>Since G is the center and the radius is 26, $GB = 10$ (as B is on \overline{AC} and G is 10 units away from \overline{AC}). Because \overline{AC} and \overline{DF} are equidistant, $GE = 10$ as well (since E is on \overline{DF} and G is 10 units away from \overline{DF}).</p> <p>Now, consider $\triangle AGB$ and $\triangle GFE$. Since $GB \perp AC$ and $GE \perp DF$, $GB = GE = 10$. Also, $GA = GF = 26$ because they are radii of the circle.</p> <p>By the Pythagorean theorem in $\triangle AGB$:</p> $AG^2 = AB^2 + GB^2, \dots, AB = 24.$ <p>Since B is the midpoint of \overline{AC}, $AC = 2 \times AB = 2 \times 24 = 48$. Similarly, in $\triangle GFE$: $FG^2 = FE^2 + GE^2, \dots, FE = 24$.</p> <p>Since E is the midpoint of \overline{DF}, $DF = 2 \times FE = 2 \times 24 = 48$, so $DE = \frac{DF}{2} = 24$.</p> <p>Thus, the answer is 24.</p> <p></think></p> <p><answer>24</answer></p>
---	---

Figure 1: A comparison of three MLLMs on a geometry problem. Both Qwen2.5-VL-7B-IT and its RLVR-trained variant make severe perception errors but manage to guess the answer, whereas our Perception-R1 first accurately describes the image and then solves the problem correctly.

learning (RL), particularly RL with Verifiable Rewards (RLVR), in enhancing advanced reasoning capabilities of LLMs and MLLMs, thereby drawing significant attention from the research community.

Motivated by these pioneering works, a growing number of studies [35, 39, 53, 19, 11] have emerged to further advance the multimodal reasoning capabilities of MLLMs leveraging RLVR, which trains MLLMs solely with rewards derived from the correctness of the final answer. For instance, MM-Eureka [35] and R1-VL [58] successfully stabilized the training of RLVR in the multimodal domain by incorporating additional training tricks and mechanisms. R1-OneVision [53] and Vision-R1 [19] first constructed a large-scale high-quality multimodal dataset by addressing the modality gap issue, then applied a training pipeline consisting of cold-start followed by RLVR to train MLLMs on the dataset. All these works effectively enhanced the multimodal reasoning capabilities of MLLMs, leading to substantial performance improvements across most benchmarks.

Multimodal reasoning can be naturally decomposed into multimodal perception and logical reasoning [2, 65], where multimodal perception is responsible for accurately understanding the multimodal input and supplying essential information for subsequent reasoning, thereby serving as the foundation for effective multimodal reasoning. Although RLVR-trained MLLMs demonstrate improved reasoning capabilities, our detailed analysis reveal that existing RLVR fails to effectively improve the multimodal perception capabilities of MLLMs, making it a major bottleneck that restricts their further advancement in multimodal reasoning. For example, as illustrated in Figure 1, the original MLLM (left in Figure 1) makes severe multimodal perception errors (e.g., referring to “right triangle $\triangle OAE$ ” that does not exist in the image), indicating its limited multimodal perception capabilities. Nevertheless, it still manage to guess the correct answer. This makes existing RLVR method, which optimize MLLMs solely based on answer accuracy, struggles to correct perception errors and may even reinforce this flawed reasoning path. Consequently, the resulting MLLM (middle in Figure 1) still exhibit weak multimodal perception capabilities similar to its original counterpart (e.g., referring to “ RG ” that does not exist), hindering the development of genuine multimodal reasoning capabilities.

We attribute this challenge to the rewards sparsity for multimodal perception when training MLLMs with existing RLVR, making it difficult to effectively enhance the multimodal perception capabilities of MLLMs. To address this challenge, we propose Perception-R1, which incorporates a novel and effective visual perception reward into the multimodal RLVR training process. The visual perception reward provides an additional reward signal beyond answer accuracy, explicitly encouraging MLLMs to perceive visual content accurately, thereby alleviating reward sparsity in RLVR training and facilitating more effective multimodal reasoning by strengthening the MLLMs’ perceptual foundation. Specifically, we introduce visual annotations into RLVR as auxiliary references, encouraging MLLMs to generate perception-accurate responses that closely align with them during training. To obtain

such visual annotations, we first collect CoT trajectories of problems with accurate final answers from state-of-the-art multimodal reasoning model, treating the visual information embedded in these correct trajectories as accurate owing to the model’s strong perception capabilities, and then employ an LLM to extract natural language visual annotations from them. During RLVR training, visual perception reward is assigned based on the consistency between the visual annotations and the responses of MLLM, as evaluated by a judging LLM via prompting. By incorporating the visual perception reward into RLVR, our Perception-R1 achieves new state-of-the-art (SOTA) performance on several multimodal math benchmarks using only 1,442 training samples, surpassing Vision-R1, which requires 200K data samples for training in total.

In summary, our contributions are threefold:

- (1). We investigate the behaviors of RLVR-trained MLLMs and their original counterparts, and find that their multimodal perception capabilities are not statistically significantly different, remaining a major bottleneck that limits further advancement in multimodal reasoning.
- (2). We propose Perception-R1, which introduces a novel visual perception reward into RLVR. By providing an additional perception reward signal, Perception-R1 alleviates the reward sparsity in multimodal perception and effectively enhances the multimodal reasoning capabilities of MLLMs.
- (3). Extensive experiments on several multimodal benchmarks demonstrate the superiority of our proposed Perception-R1, which exhibits significantly improved multimodal perception capabilities and achieves SOTA performance on most benchmarks using only 1,442 training samples.

2 Related Work

2.1 Multimodal Large Language Models

Multimodal Large Language Models (MLLMs) have witnessed rapid advancements in recent years. Most studies [4, 48, 5, 28, 9] developed MLLMs by aligning a visual encoder to a pre-trained LLM through vision-language adaptors (VL-adaptors), making the modality alignment the core of MLLMs development. Early efforts focused on architectural designs to enhance alignment, exploring various forms of VL-adaptors and visual encoders. From the perspective of VL-adaptor, three mainstream types have been widely studied: cross-attention modules [4, 10, 59], parallel visual experts [49, 13] inspired by LoRA [18], and simple linear projection layers [28, 25, 48, 5, 7]. Among these, linear projection layers have demonstrated strong effectiveness [23] and are now predominantly adopted in SOTA MLLMs. Meanwhile, CLIP-based visual encoders have been found to possess intrinsic limitations in multimodal perception [46], prompting the research of applying hybrid vision towers [46, 30] and scaling up the vision backbones [9, 8, 7]. Beyond the exploration of architecture of MLLMs, recent studies have also advanced modality alignment from a data perspective. Works such as LLaVA [28, 26, 27, 25], Qwen-VL [4, 48, 5], and InternVL [9, 8, 7] have significantly scaled up both the volume and diversity of training data. For instance, LLaVA’s training data grew from 753K samples to 9.36M in LLaVA-OV [25], while the data diversity broadened from general images to include math reasoning, document and video understanding, substantially improving VL alignment and overall performance on multimodal benchmarks.

2.2 Multimodal Large Language Models Reasoning

Since the advent of MLLMs, enhancing their complex multimodal reasoning capabilities has drawn increasing research attention. Early efforts [16, 43, 38] focused on distilling CoT trajectories from proprietary models like GPT-4V [1] and Gemini [44] to inject reasoning abilities into open-source MLLMs. Although these methods can achieve great improvement on targeted benchmarks, they lack generalizability to out-of-distribution domains. Following the introduction of test-time scaling by OpenAI-o1 [21], many works [51, 50, 54, 33] explored the implementation of it in multimodal reasoning domain. Approaches like LLaVA-CoT [51], AtomThink [50], and URSA [33] implemented o1-style reasoning by enforcing step-wise structured outputs and leveraging process-level rewards to evaluate intermediate steps. Recently, the remarkable success of DeepSeek-R1 [17] in improving LLM reasoning through large-scale RLVR has motivated researchers to transfer similar approaches into the multimodal reasoning domain. Vision-RFT [29] and R1-V [6] applied RLVR to object detection and counting tasks, significantly improving the image understanding capabilities of MLLMs. MM-Eureka [35] and MMR1 [24] extend RLVR on math reasoning tasks without cold-start, achieving substantial improvements in multimodal reasoning. Vision-R1 adopted a training

pipeline that first performs cold-start on long CoT data, then conduct large-scale RL, achieved SOTA performance on several multimodal math benchmarks. Although prior works have made remarkable progress in enhancing the multimodal reasoning abilities of MLLMs, they overlooked the multimodal perception capabilities of MLLMs, which are essential for complex multimodal reasoning and remains difficult to optimize under existing RLVR method due to sparse rewards.

3 Preliminaries

This section formulates the multimodal reasoning task (Section 3.1) and introduces key concepts of the RLVR algorithm (Section 3.2) employed in this work.

3.1 Problem Formulation

In this work, we investigate the multimodal reasoning task in the context of MLLMs. Let $\mathcal{D} = (x_1, x_2, \dots, x_N)$ be a multimodal reasoning dataset, where each data sample $x_i = (V, Q, a)$ comprises visual input V (e.g., image), a textual query Q , and the corresponding ground-truth answer a . The multimodal reasoning task is defined as follows: given a data sample $x_i \in \mathcal{D}$ as input, the MLLM is required to generate a textual token sequence y that aims to reach the ground-truth answer a .

3.2 Reinforcement Learning with Verifiable Rewards (RLVR)

Compared to previous RL algorithms [37], Reinforcement Learning with Verifiable Rewards (RLVR) eliminates the dependency on external reward models by using ground-truth answers for reward assignment, which both mitigates challenging reward hacking issues [12] and substantially reduces computational overhead. Existing methods [17, 35, 19] typically apply RLVR with two main components, including reward functions and the Group Relative Policy Optimization (GRPO) algorithm.

Reward Functions: The reward functions consist of two components:

- (1). *Format Reward* (r_f) encourages MLLMs to generate in a structured “think-then-answer” format, with the reasoning process enclosed in `<think>` tags and the answer enclosed in `<answer>` tags.
- (2). *Accuracy Reward* (r_a) drives the reasoning optimization in RLVR training by evaluating the correctness of predicted answer. Existing works [15, 19, 24] mostly adopt a symbolic system to judge the equivalence of ground-truth a and answer in MLLMs’ response y .

Since format reward r_f only enforces structured output, while accuracy reward r_a plays a central role in enhancing the multimodal reasoning capabilities of MLLMs, we refer to RLVR with a following reward function as **accuracy-only RLVR**:

$$r(y_i, a) = \alpha \cdot r_f(y_i) + \beta \cdot r_a(y_i, a) \quad (1)$$

where α, β are coefficients that control the impact of these two rewards.

Group Relative Policy Optimization (GRPO) [42] is a variant of Proximal Policy Optimization (PPO) [41], which eliminates the need for an explicit critic by estimating baseline rewards from groups of sampled rollouts, thereby reducing computational overhead while maintaining performance. For each data sample $x \in \mathcal{D}$, GRPO first samples a group of rollouts $Y = (y_1, y_2, \dots, y_G)$ from the policy model π_θ , then computes advantage \hat{A}_i by normalizing rewards across these rollouts:

$$\hat{A}_i = \frac{r(y_i, a) - \text{mean}\{r(y_1, a), r(y_2, a), \dots, r(y_G, a)\}}{\text{std}\{r(y_1, a), r(y_2, a), \dots, r(y_G, a)\}} \quad (2)$$

After obtaining the advantages, GRPO optimizes the policy model π_θ by maximizing the objective:

$$\begin{aligned} \mathcal{L}(\theta) = & \mathbb{E}_{x \in \mathcal{D}} \mathbb{E}_{\{y_i\}_{i=1}^G \sim \pi_{\theta_{\text{old}}}} \\ & \left[\frac{1}{G} \sum_{i=1}^G \frac{1}{|y_i|} \sum_{t=1}^{|y_i|} \left\{ \min \left[s_t(x, y_i) \hat{A}_i, \text{clip} (s_t(x, y_i), 1 - \varepsilon, 1 + \varepsilon) \hat{A}_i \right] - \delta \cdot \text{KL}(\pi_\theta \| \pi_{\text{ref}}) \right\} \right] \end{aligned} \quad (3)$$

where $s_t(x, y_i) = \frac{\pi_\theta(y_{i,t} | x, y_{i,<t})}{\pi_{\theta_{\text{old}}}(y_{i,t} | x, y_{i,<t})}$, ε is the clipping hyper-parameter, δ is the coefficient that controls the impact of Kullback-Leibler (KL) divergence, π_θ is the policy model and π_{ref} is the fixed reference model that is usually initialized from the initial policy.

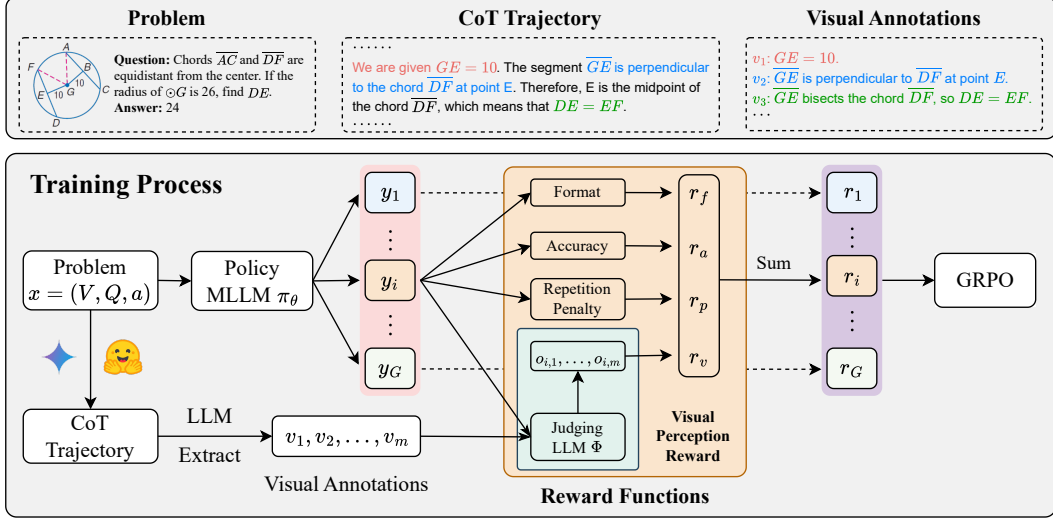


Figure 2: Overview of training pipeline of the proposed Perception-R1. In addition to the accuracy and format rewards, we introduce a novel visual perception reward that explicitly guides MLLMs toward improving their multimodal perception capabilities.

4 Methods

4.1 Accuracy-only RLVR Fails to Improve Multimodal Perception in MLLMs

Multimodal reasoning capabilities can be naturally decomposed into multimodal perception and logical reasoning capabilities [2, 65]. Although RLVR has proven effective in enhancing logical reasoning, many failure cases similar to Figure 1 reveal its limited impact on enhancing multimodal perception. To further validate this observation, we first train Qwen2-VL-7B-IT [48] and Qwen2.5-VL-7B-IT [5] on Geometry3K [32] dataset using accuracy-only RLVR, and then conduct a detailed investigation of their multimodal perception capabilities by analyzing their CoT trajectories on the MathVista [31] and MathVerse [60] benchmarks. Further details are provided in Appendix B.1.

Our investigation yields the following results:

- (1). For Qwen2-VL-7B-IT, we analyze 50 and 25 incorrect cases from MathVista and MathVerse, respectively, and find that 72% and 68% of these failures are caused by multimodal perception errors. For Qwen2.5-VL-7B-IT, the corresponding proportions are 78% and 76%, respectively. These results highlight that multimodal perception remains a major bottleneck for RLVR-trained MLLMs, which limits their further advancement in multimodal reasoning.
- (2). We conduct exact binomial variation of McNemar’s test [34, 14] on 50 multimodal problems randomly sampled from MathVista. For Qwen2-VL-7B-IT, the numbers of discordant cases related to multimodal perception are 1 and 5, respectively. For Qwen2.5-VL-7B-IT, the numbers are 2 and 4, respectively. As a result, the exact binomial test yields p -values of 0.22 and 0.69, both far above the 0.05 significance level, indicating that the multimodal perception abilities of the accuracy-only RLVR trained MLLMs do not significantly differ from those of their original counterparts.

4.2 Perception-R1

We attribute this limitation to the reward sparsity of accuracy-only RLVR, as it is challenging for an MLLM to produce a response that is both perceptually accurate and yields the correct answer for problems it fails to perceive correctly, making it difficult for accuracy-only RLVR to effectively optimize the multimodal perception capabilities of MLLMs. To tackle this issue, we propose Perception-R1, which introduces a novel and effective visual perception reward into RLVR, explicitly guiding MLLMs toward improving their multimodal perception capabilities, thereby effectively enhancing their overall multimodal reasoning performance.

Since directly introducing a multimodal reward model may introduce additional reward hacking issues, we largely adhere to the RLVR paradigm in designing the visual perception reward. As

shown in Figure 2, we first collect CoT trajectories that contain accurate visual information and then extract visual annotations from them. These visual annotations serve as references for assigning visual perception reward, analogous to the use of ground-truth answers in computing accuracy reward. Subsequently, a judging LLM is used to assess the consistency between visual annotations and the MLLM generated responses, thereby assisting in the assignment of the visual perception reward. Finally, we aggregate all rewards and apply GRPO to optimize the policy model.

4.2.1 Curation of Visual Annotations

Visual images often encode rich and complex information that is difficult to convey fully through text. Since our ultimate objective is to enhance the multimodal reasoning capabilities of MLLMs rather than to generate faithful image captions, we focus on guiding MLLMs to concentrate on visual content pertinent to problem solving, such as identifying $GE = 10$ rather than being influenced by superficial cues like line color in Figure 2.

To obtain such visual information, we employ a SOTA proprietary MLLM to generate CoT trajectories on multimodal reasoning dataset \mathcal{D} , treating the visual information embedded within these trajectories as accurate and highly relevant to problem-solving. Notably, these CoT trajectories can also be obtained from existing open-source multimodal SFT datasets. We then further prompt a strong text-only LLM to extract this embedded visual information from each CoT trajectory into a sequence of visual annotations $\mathcal{V} = (v_1, v_2, \dots, v_m)$, where each v_i represents a textual atomic visual annotation of the image that is critical for problem-solving (e.g., $GE = 10$, $\overline{GE} \perp \overline{DF}$ in Figure 2), and m denotes the total number of visual annotations within the trajectory. These visual annotations \mathcal{V} will serve as ground-truth references for evaluating whether the policy model accurately perceives visual content during RLVR training, analogous to the role of ground-truth answers in the accuracy reward.

4.2.2 Visual Perception Reward

During RLVR training, we need to evaluate the consistency between the visual annotations \mathcal{V} and the visual description embedded in the responses generated by the policy model π_θ . Since symbolic systems struggle to capture the complex semantics of natural language, we address this limitation by introducing a judging LLM Φ to assess whether each atomic visual annotation v_i is accurately reflected in the responses generated by policy model, thereby extending the source of reward signals.

Formally, given a data sample $x \in \mathcal{D}$ and its corresponding visual annotations $\mathcal{V} = (v_1, v_2, \dots, v_m)$, we first sample a response y_i from the policy model π_θ , then employ a judging LLM Φ to assess whether each atom annotation v_j is presented in y_i . Consequently, this process results in a judgment sequence $\mathcal{J} = (o_{i,1}, o_{i,2}, \dots, o_{i,m})$, where $o_{i,j} \in \{0, 1\}$ indicates whether v_j is accurately reflected in y_i or not. Obtaining \mathcal{J} , we can compute the visual perception reward r_v for y_i :

$$r_v(y_i, \mathcal{V}) = \frac{\sum\{o_{i,1}, o_{i,2}, \dots, o_{i,m}\}}{|o_{i,1}, o_{i,2}, \dots, o_{i,m}|}, \text{ where } o_{i,j} = \Phi(y_i, v_j) \in \{0, 1\}, v_j \in \mathcal{V} \quad (4)$$

Accordingly, our visual-enhanced reward function is defined as follows:

$$r(y_i, a, \mathcal{V}) = \alpha \cdot r_f(y_i) + \beta \cdot r_a(y_i, a) + \gamma \cdot r_v(y_i, \mathcal{V}) + r_p(y_i) \quad (5)$$

where r_f and r_a are format reward and accuracy reward explained in Section 3.2, γ is the coefficient that controls the impact of visual perception reward, r_p is the repetition penalty reward that discourage repetitive behavior during MLLMs' generation. The introduction of r_p is motivated by our observation that directly incorporating r_v will result in increased repetition in the generated responses, which in turn impairs the model's multimodal reasoning capabilities. Following prior works [55, 15], we implement r_p using a simple N -gram repetition penalty.

During RLVR training, we replace the reward function $r(y_i, a)$ in Eq.1 by our visual-enhanced reward $r(y_i, a, \mathcal{V})$, and train the MLLM to maximize the GRPO objective exhibited in Eq.3.

5 Experiments

5.1 Experiment Settings

Training Dataset. We adopt Geometry3K [32] dataset as our training data, which originally contains 2,101 samples for training. To obtain the visual annotations, we employ Gemini-2.5-Pro [44] to

Table 1: Performance comparison between Perception-R1 and baselines on four benchmarks. The best and second-best results of Open-Source Reasoning MLLMs are highlighted in **red** and **blue**.

Model	#Data	MathVista			MathVerse		MathVision	WeMath
		GEO	GPS	ALL	VO	ALL		
<i>Proprietary MLLMs</i>								
GPT-4o	/	-	-	63.8	-	50.2	30.4	68.8
Claude-3.7-Sonnet	/	-	-	66.8	-	52.0	41.3	72.6
Kimi-k1.5	/	-	-	74.9	-	-	38.6	-
OpenAI-o1	/	-	-	73.9	-	57.0	60.3	-
<i>Open-Source General MLLMs</i>								
Qwen2.5-VL-7B-IT	/	68.6	69.2	68.0	42.2	47.4	25.1	61.4
Qwen2.5-VL-72B-IT	/	77.4	79.8	75.8	51.1	55.8	37.9	71.9
InternVL2.5-8B	/	-	-	64.4	-	39.5	19.7	53.5
InternVL2.5-78B	/	-	-	72.3	-	51.7	32.2	66.3
InternVL3-8B	/	-	-	71.6	-	39.8	29.3	-
<i>Open-Source Reasoning MLLMs</i>								
AtomThink-8B	316K	-	-	53.3	33.1	40.5	-	-
URSA-7B	3.06M	-	79.3	59.8	28.6	45.7	-	-
R1-VL-7B	10K	-	-	63.5	-	40.0	24.7	-
R1-OneVision-7B	155K	-	-	64.1	40.0	46.4	29.9	61.8
OpenVLThinker-7B	25K	-	-	70.2	-	47.9	25.3	-
MM-Eureka-7B	15K	-	-	73.0	-	50.3	26.9	66.1
Vision-R1-7B	200K	80.3	83.2	73.5	-	52.4	-	-
Perception-R1-7B	1.4K	81.2	83.7	74.2	50.1	54.3	28.6	72.0

generate CoT trajectories on the training data and retain those with correct answers. We then use Qwen2.5-32B-IT [52] to extract visual annotations from the retained CoT trajectories. This process results in a total of 1,442 data samples with associated visual annotations.

Benchmarks and Evalution Settings. For comprehensive evaluation, we evaluate Perception-R1 on diverse challenging multimodal reasoning benchmarks, including MathVista [31], MathVerse [60], MathVision [47] and WeMath [40]. During inference, we use vLLM [22] library for efficiency and apply greedy decoding with a temperature of 0.0.

Baselines. We compare our method against several powerful MLLMs: **(1) Proprietary MLLMs:** GPT-4o [20], OpenAI-o1 [21], Claude-3.7-Sonnet [3], Kimi-k1.5 [45], **(2) Open-Source General MLLMs:** Qwen2.5-VL-7B-IT, Qwen2.5-VL-72B-IT [5], InternVL2.5-8B, InternVL2.5-78B [7], InternVL3-8B [66], **(3) Open-Source Reasoning MLLMs:** AtomThink-8B[50], URSA-7B [33], R1-OneVision [53], R1-VL [58], OpenVLThinker [11], MM-Eureka-7B [35], Vision-R1 [19].

Implementation Details. In the experiments, we adopt Qwen2.5-VL-7B-IT [5] as our base model and train it using the EasyR1 [64] framework. During training, we adopt Qwen2.5-32B-IT [52] as the judging LLM and set the learning rate to 1e-6 with a warmup ratio of 0.05. The model is trained for a total of 25 epochs with a batch size of 128. Following prior works [35, 56], we remove the KL penalty from Eq.3 during RL training to achieve better performance, i.e., $\delta = 0$. Additionally, the coefficients in Eq.5 are set to $\alpha = 0.1$, $\beta = 0.9$, and $\gamma = 0.7$, respectively. The training process takes about 16 hours on 16 NVIDIA-A800-80G GPUs. All prompts can be found in Appendix C.

5.2 Main Results

We present the performance comparison between our Perception-R1 and existing SOTA methods across multiple benchmarks in Table 1. The performance of applying our method on Qwen2-VL-7B-IT is presented in Appendix B.2. We summarize our findings as follows:

Our Perception-R1 achieves new SOTA performance on most of the benchmarks. As demonstrated in the table, despite being trained on a small dataset of only 1,442 samples, our Perception-R1

Table 2: Component & approach ablation studies of Perception-R1. The best result is marked in red.

Model	MathVista			MathVerse		MathVision	WeMath
	GEO	GPS	ALL	VO	ALL		
Qwen2.5-VL-7B-IT	68.6	69.2	68.0	42.2	47.4	25.1	61.4
+ Accuracy-only RLVR	73.2	74.5	73.3	47.1	51.3	26.6	69.5
<i>Component Ablations</i>							
+ Visual Perception Reward	74.0	76.0	73.6	48.1	52.6	26.9	68.5
+ Repetition Penalty	74.1	76.4	73.6	47.3	53.0	27.6	70.4
<i>Approach Ablations</i>							
SFT	68.2	68.8	66.7	35.4	39.3	20.5	53
Qwen2.5-VL-32B-IT as RM	78.2	80.8	73.1	49.3	54.0	27.2	66.0
Perception-R1-7B	81.2	83.7	74.2	50.1	54.3	28.6	72.0

still achieves remarkable performance across all benchmarks, outperforming previous SOTA methods, InternVL2.5-78B and GPT-4o on all benchmarks except MathVision. We also conduct statistical significance testing using a one-sample t-test, finding that the average improvement is significant with $p < 0.05$ compared to Vision-R1-7B, and $p < 0.01$ compared to MM-Eureka-7B. This result provides strong evidence for the effectiveness of our proposed Perception-R1. It also underscores the critical role of multimodal perception in enabling effective multimodal reasoning, suggesting that accuracy-only RLVR requires further adaptation when applied to the multimodal reasoning domain. On MathVision, although Perception-R1 achieves substantial improvements over the base model (28.6% vs. 25.1%), there remains a small gap compared to R1-OneVision. We attribute this to the data distribution gap between our training dataset and MathVision, and we believe this can be mitigated in the future by scaling up both the quantity and diversity of training data.

The multimodal perception capabilities of Perception-R1 show tangible improvements. On the “Vision-Only” (VO) set of MathVerse, Perception-R1 outperforms both baselines and original MLLM by a large margin, and even achieves performance comparable to Qwen2.5-VL-72B-IT (50.1% vs. 51.1%), demonstrating its superior capabilities in multimodal perception. To ensure a more rigorous conclusion, we also conduct McNemar’s test on Perception-R1. We investigate the same 50 problems as presented in Section 4.1 and find that the numbers of discordant cases for multimodal perception are 2 and 10, respectively. As a result, the exact binomial variation of McNemar’s test [34] yields exact p value of 0.04, below the 0.05 significance threshold, indicating that the multimodal perception capabilities of Perception-R1 is substantially improved compared to the original MLLM.

Perception-R1 effectively enhances multimodal reasoning capabilities of MLLMs in a highly data-efficient manner. Although existing methods such as MM-Eureka [35] and Vision-R1 [19] have demonstrated strong data efficiency in enhancing the multimodal reasoning capabilities of MLLMs compared to prior SFT and PRM approaches [50, 33], our Perception-R1 achieves even better performance using over $100\times$ less data than Vision-R1 and $10\times$ less data than MM-Eureka, demonstrating its exceptional data efficiency in developing reasoning MLLMs. This finding suggests that data efficiency can be substantially improved by incorporating richer reward signals from data beyond the final answer, as demonstrated by our proposed visual perception rewards.

5.3 Ablation Study

In this section, we conduct ablation studies from two perspectives: (1) evaluating the effectiveness of each component of Perception-R1, i.e., the visual perception reward and the repetition penalty; and (2) comparing Perception-R1 with alternative approaches, including directly using an MLLM as the reward model and employing supervised fine-tuning to train the base model.

We present the results of ablation studies in Table 2. As shown in the table, firstly, the accuracy across all benchmarks declines when either the visual perception reward or the repetition penalty is removed, demonstrating the effectiveness and necessity of both components in our Perception-R1. Secondly, all ablations incorporating visual perception reward outperform others that are trained

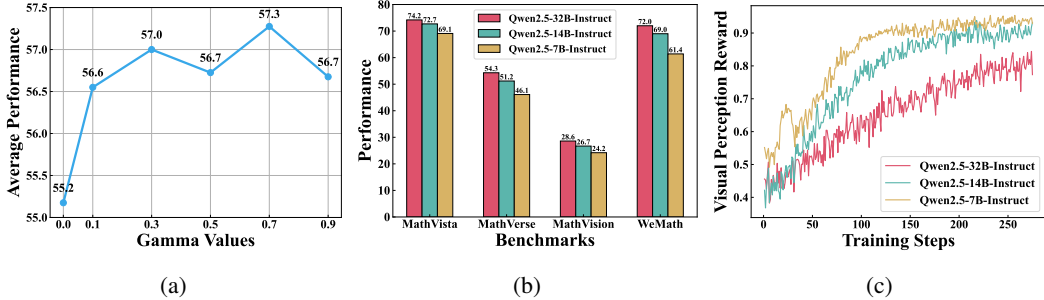


Figure 3: (a). Average performance across all benchmarks with varying γ values. (b). Comparison of performance across all benchmarks when using different judging LLMs. (c). Dynamics of visual perception reward during training when using different judging LLMs.

with accuracy-only RLVR on the “Vision Only” (VO) subset of MathVerse, further indicating that our proposed visual perception reward enhances the multimodal perception capabilities of MLLMs. Thirdly, directly employing a powerful MLLM (Qwen2.5-VL-32B-IT) as the reward model does not yield better performance than our Perception-R1. We attribute this to reward hacking (See Appendix B.3), which underscores the importance of constructing verifiable visual annotations. To demonstrate the effectiveness of our overall RL training pipeline, we also conduct SFT experiment on the base model using the same 1,442 CoT trajectories distilled from Gemini-2.5-Pro [44]. From Table 2, it is observed that the SFT model yields inferior performance, with results on all benchmarks falling short of those of the base model after training. This phenomenon highlights the superior generalization ability and data efficiency of Perception-R1 compared to supervised fine-tuning.

5.4 Further Analysis of Visual Perception Reward

To further explore the dynamics of the visual perception reward, we conduct experiments by varying the coefficient γ in Eq. 5 and evaluating the impact of different judging LLMs.

To study the impact of coefficient γ , we train a series of models with $\gamma \in \{0, 0.1, 0.3, 0.5, 0.7, 0.9\}$, and present their average performance across all benchmarks in Figure 3a. We observe that models trained with different values of γ achieve comparable performance across all benchmarks, while all significantly outperform the model that does not incorporate the visual perception reward. The result suggests that only a small amount of visual optimization signal is sufficient to effectively incentivize the multimodal perception and reasoning capabilities of MLLMs, and increasing the value of γ does not lead to significantly better results. We attribute this to GRPO, which normalizes the advantages across responses that receive different visual perception rewards when other rewards are identical.

Given that the judging LLM plays a central role in assigning visual perception rewards, we investigate how its capability affects the performance of the resulting MLLM. Specifically, we employ Qwen2.5 [52] models of varying sizes as judging LLMs to train Qwen2.5-VL-7B-IT with γ fixed at 0.7. The performance of the resulting models across all benchmarks is presented in Figure 3b. As the capabilities of the judging LLMs decrease, the performance of the resulting MLLM consistently deteriorates, with the model trained using the 7B judging LLM even underperforming the original MLLM on MathVerse (46.1% vs. 47.4%) and MathVision (24.2% vs. 25.1%). According to the training dynamics of visual perception reward presented in Figure 3c, the reward increases rapidly and saturates early when using weak judging LLMs, implying the presence of severe reward hacking issues that misguide the resulting MLLM away from accurate problem solving.

6 Conclusion

In this paper, we first conduct McNemar’s test on accuracy-only RLVR-trained MLLMs and find no statistically significant improvement in their multimodal perception capabilities compared to their original counterparts, which consequently limits their further advancement in multimodal reasoning. To address this limitation, we propose Perception-R1, which introduces a novel visual perception reward in addition to the standard accuracy reward, explicitly encouraging accurate visual perception

during RLVR training. Specifically, we first collect textual visual annotations from CoT trajectories as references, and then assign visual perception reward by evaluating the consistency between these annotations and MLLM-generated response using a judging LLM. Extensive experiments demonstrate the effectiveness of Perception-R1, achieving new SOTA performance on several multimodal math benchmarks using only 1,442 training samples.

References

- [1] Josh Achiam, Steven Adler, Sandhini Agarwal, Lama Ahmad, Ilge Akkaya, Florencia Leoni Aleman, Diogo Almeida, Janko Altenschmidt, Sam Altman, Shyamal Anadkat, et al. Gpt-4 technical report. *arXiv preprint arXiv:2303.08774*, 2023.
- [2] Saeed Amizadeh, Hamid Palangi, Alex Polozov, Yichen Huang, and Kazuhito Koishida. Neuro-symbolic visual reasoning: Disentangling. In *International Conference on Machine Learning*, pages 279–290. Pmlr, 2020.
- [3] Anthropic. Claude 3.5 sonnet. <https://www.anthropic.com/news/clause-3-5-sonnet>, 2024.
- [4] Jinze Bai, Shuai Bai, Shusheng Yang, Shijie Wang, Sinan Tan, Peng Wang, Junyang Lin, Chang Zhou, and Jingren Zhou. Qwen-vl: A versatile vision-language model for understanding, localization, text reading, and beyond. *arXiv preprint arXiv:2308.12966*, 2023.
- [5] Shuai Bai, Keqin Chen, Xuejing Liu, Jialin Wang, Wenbin Ge, Sibo Song, Kai Dang, Peng Wang, Shijie Wang, Jun Tang, Humen Zhong, Yuanzhi Zhu, Mingkun Yang, Zhaohai Li, Jianqiang Wan, Pengfei Wang, Wei Ding, Zheren Fu, Yiheng Xu, Jiabo Ye, Xi Zhang, Tianbao Xie, Zesen Cheng, Hang Zhang, Zhibo Yang, Haiyang Xu, and Junyang Lin. Qwen2.5-vl technical report. *arXiv preprint arXiv:2502.13923*, 2025.
- [6] Liang Chen, Lei Li, Haozhe Zhao, Yifan Song, and Vinci. R1-v: Reinforcing super generalization ability in vision-language models with less than \$3. <https://github.com/Deep-Agent/R1-V>, 2025.
- [7] Zhe Chen, Weiyun Wang, Yue Cao, Yangzhou Liu, Zhangwei Gao, Erfei Cui, Jinguo Zhu, Shenglong Ye, Hao Tian, Zhaoyang Liu, et al. Expanding performance boundaries of open-source multimodal models with model, data, and test-time scaling. *arXiv preprint arXiv:2412.05271*, 2024.
- [8] Zhe Chen, Weiyun Wang, Hao Tian, Shenglong Ye, Zhangwei Gao, Erfei Cui, Wenwen Tong, Kongzhi Hu, Jiapeng Luo, Zheng Ma, et al. How far are we to gpt-4v? closing the gap to commercial multimodal models with open-source suites. *arXiv preprint arXiv:2404.16821*, 2024.
- [9] Zhe Chen, Jiannan Wu, Wenhui Wang, Weijie Su, Guo Chen, Sen Xing, Muyan Zhong, Qinglong Zhang, Xizhou Zhu, Lewei Lu, et al. Internvl: Scaling up vision foundation models and aligning for generic visual-linguistic tasks. In *Proceedings of the IEEE/CVF conference on computer vision and pattern recognition*, pages 24185–24198, 2024.
- [10] Wenliang Dai, Junnan Li, Dongxu Li, Anthony Meng Huat Tiong, Junqi Zhao, Weisheng Wang, Boyang Albert Li, Pascale Fung, and Steven C. H. Hoi. Instructblip: Towards general-purpose vision-language models with instruction tuning. *ArXiv*, abs/2305.06500, 2023.
- [11] Yihe Deng, Hritik Bansal, Fan Yin, Nanyun Peng, Wei Wang, and Kai-Wei Chang. Open-vlthinker: An early exploration to complex vision-language reasoning via iterative self-improvement. *arXiv preprint arXiv:2503.17352*, 2025.
- [12] Carson Denison, Monte MacDiarmid, Fazl Barez, David Duvenaud, Shauna Kravec, Samuel Marks, Nicholas Schiefer, Ryan Soklaski, Alex Tamkin, Jared Kaplan, et al. Sycophancy to subterfuge: Investigating reward-tampering in large language models. *arXiv preprint arXiv:2406.10162*, 2024.

[13] Xiaoyi Dong, Pan Zhang, Yuhang Zang, Yuhang Cao, Bin Wang, Linke Ouyang, Xilin Wei, Songyang Zhang, Haodong Duan, Maosong Cao, et al. Internlm-xcomposer2: Mastering free-form text-image composition and comprehension in vision-language large model. *arXiv preprint arXiv:2401.16420*, 2024.

[14] Allen L. Edwards. Note on the “correction for continuity” in testing the significance of the difference between correlated proportions. *Psychometrika*, 13(3):185–187, 1948.

[15] Hugging Face. Open r1: A fully open reproduction of deepseek-r1, January 2025.

[16] Jiahui Gao, Renjie Pi, Jipeng Zhang, Jiacheng Ye, Wanjun Zhong, Yufei Wang, Lanqing Hong, Jianhua Han, Hang Xu, Zhenguo Li, et al. G-llava: Solving geometric problem with multi-modal large language model. *arXiv preprint arXiv:2312.11370*, 2023.

[17] Daya Guo, Dejian Yang, Haowei Zhang, Junxiao Song, Ruoyu Zhang, Runxin Xu, Qihao Zhu, Shirong Ma, Peiyi Wang, Xiao Bi, et al. Deepseek-r1: Incentivizing reasoning capability in llms via reinforcement learning. *arXiv preprint arXiv:2501.12948*, 2025.

[18] Edward J Hu, Yelong Shen, Phillip Wallis, Zeyuan Allen-Zhu, Yuanzhi Li, Shean Wang, Lu Wang, Weizhu Chen, et al. Lora: Low-rank adaptation of large language models. *ICLR*, 1(2):3, 2022.

[19] Wenxuan Huang, Bohan Jia, Zijie Zhai, Shaosheng Cao, Zheyu Ye, Fei Zhao, Yao Hu, and Shaohui Lin. Vision-r1: Incentivizing reasoning capability in multimodal large language models. *arXiv preprint arXiv:2503.06749*, 2025.

[20] Aaron Hurst, Adam Lerer, Adam P Goucher, Adam Perelman, Aditya Ramesh, Aidan Clark, AJ Ostrow, Akila Welihinda, Alan Hayes, Alec Radford, et al. Gpt-4o system card. *arXiv preprint arXiv:2410.21276*, 2024.

[21] Aaron Jaech, Adam Kalai, Adam Lerer, Adam Richardson, Ahmed El-Kishky, Aiden Low, Alec Helyar, Aleksander Madry, Alex Beutel, Alex Carney, et al. Openai o1 system card. *arXiv preprint arXiv:2412.16720*, 2024.

[22] Woosuk Kwon, Zhuohan Li, Siyuan Zhuang, Ying Sheng, Lianmin Zheng, Cody Hao Yu, Joseph E. Gonzalez, Hao Zhang, and Ion Stoica. Efficient memory management for large language model serving with pagedattention. In *Proceedings of the ACM SIGOPS 29th Symposium on Operating Systems Principles*, 2023.

[23] Hugo Laurençon, Léo Tronchon, Matthieu Cord, and Victor Sanh. What matters when building vision-language models? *Advances in Neural Information Processing Systems*, 37:87874–87907, 2024.

[24] Sicong Leng*, Jing Wang*, Jiaxi Li*, Hao Zhang*, Zhiqiang Hu, Boqiang Zhang, Hang Zhang, Yuming Jiang, Xin Li, Deli Zhao, Fan Wang, Yu Rong, Aixin Sun†, and Shijian Lu†. Mmr1: Advancing the frontiers of multimodal reasoning. <https://github.com/LengSicong/MMR1>, 2025.

[25] Bo Li, Yuanhan Zhang, Dong Guo, Renrui Zhang, Feng Li, Hao Zhang, Kaichen Zhang, Peiyuan Zhang, Yanwei Li, Ziwei Liu, et al. Llava-onevision: Easy visual task transfer. *arXiv preprint arXiv:2408.03326*, 2024.

[26] Haotian Liu, Chunyuan Li, Yuheng Li, and Yong Jae Lee. Improved baselines with visual instruction tuning. In *Proceedings of the IEEE/CVF Conference on Computer Vision and Pattern Recognition*, pages 26296–26306, 2024.

[27] Haotian Liu, Chunyuan Li, Yuheng Li, Bo Li, Yuanhan Zhang, Sheng Shen, and Yong Jae Lee. Llava-next: Improved reasoning, ocr, and world knowledge, January 2024.

[28] Haotian Liu, Chunyuan Li, Qingyang Wu, and Yong Jae Lee. Visual instruction tuning. In A. Oh, T. Naumann, A. Globerson, K. Saenko, M. Hardt, and S. Levine, editors, *Advances in Neural Information Processing Systems*, volume 36, pages 34892–34916. Curran Associates, Inc., 2023.

[29] Ziyu Liu, Zeyi Sun, Yuhang Zang, Xiaoyi Dong, Yuhang Cao, Haodong Duan, Dahua Lin, and Jiaqi Wang. Visual-rft: Visual reinforcement fine-tuning. *arXiv preprint arXiv:2503.01785*, 2025.

[30] Haoyu Lu, Wen Liu, Bo Zhang, Bingxuan Wang, Kai Dong, Bo Liu, Jingxiang Sun, Tongzheng Ren, Zhuoshu Li, Hao Yang, et al. Deepseek-vl: towards real-world vision-language understanding. *arXiv preprint arXiv:2403.05525*, 2024.

[31] Pan Lu, Hritik Bansal, Tony Xia, Jiacheng Liu, Chunyuan Li, Hannaneh Hajishirzi, Hao Cheng, Kai-Wei Chang, Michel Galley, and Jianfeng Gao. Mathvista: Evaluating mathematical reasoning of foundation models in visual contexts. In *International Conference on Learning Representations (ICLR)*, 2024.

[32] Pan Lu, Ran Gong, Shibiao Jiang, Liang Qiu, Siyuan Huang, Xiaodan Liang, and Song-chun Zhu. Inter-gps: Interpretable geometry problem solving with formal language and symbolic reasoning. In *Proceedings of the 59th Annual Meeting of the Association for Computational Linguistics and the 11th International Joint Conference on Natural Language Processing (Volume 1: Long Papers)*, pages 6774–6786, 2021.

[33] Ruilin Luo, Zhuofan Zheng, Yifan Wang, Yiyao Yu, Xinzhe Ni, Zicheng Lin, Jin Zeng, and Yujiu Yang. Ursu: Understanding and verifying chain-of-thought reasoning in multimodal mathematics. *arXiv preprint arXiv:2501.04686*, 2025.

[34] Quinn McNemar. Note on the sampling error of the difference between correlated proportions or percentages. *Psychometrika*, 12(2):153–157, 1947.

[35] Fanqing Meng, Lingxiao Du, Zongkai Liu, Zhixiang Zhou, Quanfeng Lu, Daocheng Fu, Botian Shi, Wenhui Wang, Junjun He, Kaipeng Zhang, et al. Mm-eureka: Exploring visual aha moment with rule-based large-scale reinforcement learning. *arXiv preprint arXiv:2503.07365*, 2025.

[36] Chancharik Mitra, Brandon Huang, Trevor Darrell, and Roei Herzig. Compositional chain-of-thought prompting for large multimodal models. In *Proceedings of the IEEE/CVF Conference on Computer Vision and Pattern Recognition*, pages 14420–14431, 2024.

[37] Long Ouyang, Jeffrey Wu, Xu Jiang, Diogo Almeida, Carroll Wainwright, Pamela Mishkin, Chong Zhang, Sandhini Agarwal, Katarina Slama, Alex Ray, et al. Training language models to follow instructions with human feedback. *Advances in neural information processing systems*, 35:27730–27744, 2022.

[38] Shuai Peng, Di Fu, Liangcai Gao, Xiuqin Zhong, Hongguang Fu, and Zhi Tang. Multi-math: Bridging visual and mathematical reasoning for large language models. *arXiv preprint arXiv:2409.00147*, 2024.

[39] Yingzhe Peng, Gongrui Zhang, Miaosen Zhang, Zhiyuan You, Jie Liu, Qipeng Zhu, Kai Yang, Xingzhong Xu, Xin Geng, and Xu Yang. Lmm-r1: Empowering 3b lmms with strong reasoning abilities through two-stage rule-based rl. *arXiv preprint arXiv:2503.07536*, 2025.

[40] Runqi Qiao, Qiuna Tan, Guanting Dong, Minhui Wu, Chong Sun, Xiaoshuai Song, Zhuoma GongQue, Shanglin Lei, Zhe Wei, MiaoXuan Zhang, et al. We-math: Does your large multimodal model achieve human-like mathematical reasoning? *arXiv preprint arXiv:2407.01284*, 2024.

[41] John Schulman, Filip Wolski, Prafulla Dhariwal, Alec Radford, and Oleg Klimov. Proximal policy optimization algorithms. *arXiv preprint arXiv:1707.06347*, 2017.

[42] Zhihong Shao, Peiyi Wang, Qihao Zhu, Runxin Xu, Junxiao Song, Xiao Bi, Haowei Zhang, Mingchuan Zhang, YK Li, Y Wu, et al. Deepseekmath: Pushing the limits of mathematical reasoning in open language models. *arXiv preprint arXiv:2402.03300*, 2024.

[43] Wenhao Shi, Zhiqiang Hu, Yi Bin, Junhua Liu, Yang Yang, See-Kiong Ng, Lidong Bing, and Roy Ka-Wei Lee. Math-llava: Bootstrapping mathematical reasoning for multimodal large language models. *arXiv preprint arXiv:2406.17294*, 2024.

[44] Gemini Team, Rohan Anil, Sebastian Borgeaud, Jean-Baptiste Alayrac, Jiahui Yu, Radu Soricut, Johan Schalkwyk, Andrew M Dai, Anja Hauth, Katie Millican, et al. Gemini: a family of highly capable multimodal models. *arXiv preprint arXiv:2312.11805*, 2023.

[45] Kimi Team, Angang Du, Bofei Gao, Bowei Xing, Changjiu Jiang, Cheng Chen, Cheng Li, Chenjun Xiao, Chenzhuang Du, Chonghua Liao, et al. Kimi k1. 5: Scaling reinforcement learning with llms. *arXiv preprint arXiv:2501.12599*, 2025.

[46] Shengbang Tong, Zhuang Liu, Yuexiang Zhai, Yi Ma, Yann LeCun, and Saining Xie. Eyes wide shut? exploring the visual shortcomings of multimodal llms. In *Proceedings of the IEEE/CVF Conference on Computer Vision and Pattern Recognition*, pages 9568–9578, 2024.

[47] Ke Wang, Junting Pan, Weikang Shi, Zimu Lu, Houxing Ren, Aojun Zhou, Mingjie Zhan, and Hongsheng Li. Measuring multimodal mathematical reasoning with math-vision dataset. In *The Thirty-eight Conference on Neural Information Processing Systems Datasets and Benchmarks Track*, 2024.

[48] Peng Wang, Shuai Bai, Sinan Tan, Shijie Wang, Zhihao Fan, Jinze Bai, Keqin Chen, Xuejing Liu, Jialin Wang, Wenbin Ge, Yang Fan, Kai Dang, Mengfei Du, Xuancheng Ren, Rui Men, Dayiheng Liu, Chang Zhou, Jingren Zhou, and Junyang Lin. Qwen2-vl: Enhancing vision-language model’s perception of the world at any resolution. *arXiv preprint arXiv:2409.12191*, 2024.

[49] Weihan Wang, Qingsong Lv, Wenmeng Yu, Wenyi Hong, Ji Qi, Yan Wang, Junhui Ji, Zhuoyi Yang, Lei Zhao, Song XiXuan, et al. Cogylm: Visual expert for pretrained language models. *Advances in Neural Information Processing Systems*, 37:121475–121499, 2024.

[50] Kun Xiang, Zhili Liu, Zihao Jiang, Yunshuang Nie, Runhui Huang, Haoxiang Fan, Hanhui Li, Weiran Huang, Yihan Zeng, Jianhua Han, et al. Atomthink: A slow thinking framework for multimodal mathematical reasoning. *arXiv preprint arXiv:2411.11930*, 2024.

[51] Guowei Xu, Peng Jin, Li Hao, Yibing Song, Lichao Sun, and Li Yuan. Llava-o1: Let vision language models reason step-by-step. *arXiv preprint arXiv:2411.10440*, 2024.

[52] An Yang, Baosong Yang, Beichen Zhang, Binyuan Hui, Bo Zheng, Bowen Yu, Chengyuan Li, Dayiheng Liu, Fei Huang, Haoran Wei, Huan Lin, Jian Yang, Jianhong Tu, Jianwei Zhang, Jianxin Yang, Jiaxi Yang, Jingren Zhou, Junyang Lin, Kai Dang, Keming Lu, Keqin Bao, Kexin Yang, Le Yu, Mei Li, Mingfeng Xue, Pei Zhang, Qin Zhu, Rui Men, Runji Lin, Tianhao Li, Tingyu Xia, Xingzhang Ren, Xuancheng Ren, Yang Fan, Yang Su, Yichang Zhang, Yu Wan, Yuqiong Liu, Zeyu Cui, Zhenru Zhang, and Zihan Qiu. Qwen2.5 technical report. *arXiv preprint arXiv:2412.15115*, 2024.

[53] Yi Yang, Xiaoxuan He, Hongkun Pan, Xiyan Jiang, Yan Deng, Xingtao Yang, Haoyu Lu, Dacheng Yin, Fengyun Rao, Minfeng Zhu, et al. R1-onevision: Advancing generalized multimodal reasoning through cross-modal formalization. *arXiv preprint arXiv:2503.10615*, 2025.

[54] Huanjin Yao, Jiaxing Huang, Wenhao Wu, Jingyi Zhang, Yibo Wang, Shunyu Liu, Yingjie Wang, Yuxin Song, Haocheng Feng, Li Shen, et al. Mulberry: Empowering mllm with o1-like reasoning and reflection via collective monte carlo tree search. *arXiv preprint arXiv:2412.18319*, 2024.

[55] Edward Yeo, Yuxuan Tong, Morry Niu, Graham Neubig, and Xiang Yue. Demystifying long chain-of-thought reasoning in llms. *arXiv preprint arXiv:2502.03373*, 2025.

[56] Qiying Yu, Zheng Zhang, Ruofei Zhu, Yufeng Yuan, Xiaochen Zuo, Yu Yue, Tiantian Fan, Gaohong Liu, Lingjun Liu, Xin Liu, et al. Dapo: An open-source llm reinforcement learning system at scale. *arXiv preprint arXiv:2503.14476*, 2025.

[57] Daoan Zhang, Junming Yang, Hanjia Lyu, Zijian Jin, Yuan Yao, Mingkai Chen, and Jiebo Luo. Cocot: Contrastive chain-of-thought prompting for large multimodal models with multiple image inputs. *arXiv preprint arXiv:2401.02582*, 2024.

[58] Jingyi Zhang, Jiaxing Huang, Huanjin Yao, Shunyu Liu, Xikun Zhang, Shijian Lu, and Dacheng Tao. R1-vl: Learning to reason with multimodal large language models via step-wise group relative policy optimization. *arXiv preprint arXiv:2503.12937*, 2025.

[59] Pan Zhang, Xiaoyi Dong, Bin Wang, Yuhang Cao, Chao Xu, Linke Ouyang, Zhiyuan Zhao, Haodong Duan, Songyang Zhang, Shuangrui Ding, et al. Internlm-xcomposer: A vision-language large model for advanced text-image comprehension and composition. *arXiv preprint arXiv:2309.15112*, 2023.

[60] Renrui Zhang, Dongzhi Jiang, Yichi Zhang, Haokun Lin, Ziyu Guo, Pengshuo Qiu, Aojun Zhou, Pan Lu, Kai-Wei Chang, Yu Qiao, et al. Mathverse: Does your multi-modal lilm truly see the diagrams in visual math problems? In *European Conference on Computer Vision*, pages 169–186. Springer, 2024.

[61] Renrui Zhang, Xinyu Wei, Dongzhi Jiang, Ziyu Guo, Shicheng Li, Yichi Zhang, Chengzhuo Tong, Jiaming Liu, Aojun Zhou, Bin Wei, et al. Mavis: Mathematical visual instruction tuning with an automatic data engine. *arXiv preprint arXiv:2407.08739*, 2024.

[62] Zhuosheng Zhang, Aston Zhang, Mu Li, Hai Zhao, George Karypis, and Alex Smola. Multimodal chain-of-thought reasoning in language models. *arXiv preprint arXiv:2302.00923*, 2023.

[63] Ge Zheng, Bin Yang, Jiajin Tang, Hong-Yu Zhou, and Sibei Yang. Ddcot: Duty-distinct chain-of-thought prompting for multimodal reasoning in language models. *Advances in Neural Information Processing Systems*, 36:5168–5191, 2023.

[64] Yaowei Zheng, Junting Lu, Shenzhi Wang, Zhangchi Feng, Dongdong Kuang, and Yuwen Xiong. Easyl1: An efficient, scalable, multi-modality rl training framework. <https://github.com/hiyouga/EasyR1>, 2025.

[65] Jingqi Zhou, Sheng Wang, Jingwei Dong, Lei Li, Jiahui Gao, Lingpeng Kong, and Chuan Wu. Proreason: Multi-modal proactive reasoning with decoupled eyesight and wisdom. *arXiv preprint arXiv:2410.14138*, 2024.

[66] Jinguo Zhu, Weiyun Wang, Zhe Chen, Zhaoyang Liu, Shenglong Ye, Lixin Gu, Yuchen Duan, Hao Tian, Weijie Su, Jie Shao, et al. Internvl3: Exploring advanced training and test-time recipes for open-source multimodal models. *arXiv preprint arXiv:2504.10479*, 2025.

A Benchmarks and Baselines

A.1 Benchmarks

- **MathVista** [31] MathVista is a consolidated benchmark for multimodal mathematical reasoning. We evaluate our Perception-R1 and all baselines on `testmini` split of MathVista, which consists of five subtasks: Textbook Question Answering, Visual Question Answering, Geometry Problem Solving, Math Word Problems and Figure Question Answering.
- **MathVerse** [60] MathVerse is a benchmark designed to evaluate the reasoning capabilities of MLLMs under varying proportions of textual and visual information. We evaluate our Perception-R1 and all baselines on `testmini` split of MathVerse, which includes 5 subset: Text Dominant (TD), Text Lite (TL), Vision Intensive (VI), Vision Dominant (VD), and Vision Only (VO). MathVerse covers three subtasks: “Plane Geometry” with 2,550 problems, “Functions” with 795 problems and “Solid Geometry” with 595 problems.
- **MathVision** [47] MathVision consists of 3,040 high quality mathematical problems with visual contexts sourced from real math competitions. We evaluate our Perception-R1 and all baselines on `test` split of MathVision, which includes five difficulty levels and 16 subtasks.
- **WeMath** [40] WeMath is the benchmark specifically designed to explore the problem-solving principles beyond the end-to-end performance, spanning 67 hierarchical knowledge concepts and 5 layers of knowledge granularity. We evaluate our Perception-R1 and all baselines on `testmini` split of WeMath under the multiple-choice setting.

A.2 Baselines

- **AtomThink-8B** [50] AtomThink enhances multimodal reasoning capabilities of MLLMs by emulating human-like “slow thinking” behaviors through an SFT approach. It encourages MLLMs to generate step-by-step solutions and introduces a process reward model (PRM) to evaluate the quality of each intermediate step and provide feedback to the MLLMs.
- **URSA-7B** [33] URSA also enhances the multimodal reasoning capabilities of MLLMs through an SFT approach. It employs a three-part data synthesis strategy to construct a high-quality CoT reasoning dataset for fine-tuning. URSA further incorporates a dual-view trajectory labeling approach, resulting in the DualMath-1.1M dataset, and trains a PRM to achieve inference-time scaling.
- **R1-VL** [58] R1-VL proposes a new online reinforcement learning framework StepGRPO, which enables MLLMs to self-improve reasoning ability via simple, effective and dense step-wise rewarding. It consists of two dense reasoning rewards: StepRAR and StepRVR. StepRAR is used to reward the accurate intermediate reasoning steps and StepRVR is used to reward the well-structure of the overall reasoning path.
- **R1-OneVision** [53] R1-OneVision adopts a cold-start then RL training pipeline to enhance the reasoning capabilities of MLLMs. It first addresses the modality gap to construct a high-quality long CoT multimodal dataset for cold-start initialization, then applied accuracy-only RLVR on 10K randomly sampled data to further incentivize MLLM’s reasoning abilities.
- **OpenVLThinker-7B** [11] OpenVLThinker adopts an approach that iteratively leverages SFT on lightweight training data and RL to improve reasoning capabilities of MLLMs. During the training pipeline, OpenVLThinker progressively evolves the data across iterations, retaining more challenging examples for later stages of training.
- **MM-Eureka-7B** [35] MM-Eureka constructs the MMK12 dataset, which contains 15,616 high quality multimodal reasoning data, and directly applies accuracy-only RLVR on this dataset. To stabilize and improve training, MM-Eureka incorporates several techniques during RL, including online data filtering, the removal of KL penalty, and a two-stage training strategy.
- **Vision-R1-7B** [19] Vision-R1 adopts a two-stage pipeline consisting of cold-start initialization followed by reinforcement learning to enhance the multimodal reasoning capabilities of MLLMs. It first employs powerful MLLMs and DeepSeek-R1 [17] to fill the modality gap and curate 200K multimodal CoT data for cold-start initialization. In the second stage, Vision-R1 applies accuracy-only RLVR on an additional 10K math problems, incorporating the proposed Progressive Thinking Suppression Training (PTST) technique.

Table 3: Confusion matrix of Qwen2-VL-7B-IT evaluated on \mathcal{D}_e .

	Correct Answer	Wrong Answer
Correct Perception	15	4
Wrong Perception	4	27

Table 4: Confusion matrix of accuracy-only RLVR trained Qwen2-VL-7B-IT evaluated on \mathcal{D}_e .

	Correct Answer	Wrong Answer
Correct Perception	23	0
Wrong Perception	5	22

B Further Results

B.1 Details of Analysis of Accuracy-only RLVR-trained MLLMs

In this section, we present additional details and results to the analysis in Section 4.1.

We conduct our investigation from the following two perspectives: (1) The proportion of incorrect solving cases attributable to multimodal perception errors, and (2) a comparative analysis of the multimodal perception capabilities between the RLVR-trained MLLMs and their original counterparts. The former helps identify the bottleneck in the multimodal reasoning abilities of MLLMs, while the latter assesses whether their perception capabilities improve after accuracy-only RLVR training.

Specifically, we first train Qwen2-VL-7B-IT [48] and Qwen2.5-VL-7B-IT [5] models on Geometry3K [32] dataset using accuracy-only RLVR. We then manually assess their CoT trajectories on the geometry reasoning subset of MathVista [31], as well as the “Visual Dominant” and “Visual Only” subsets of MathVerse [60]. These problems require both strong multimodal perception and logical reasoning capabilities, making them suitable for identifying potential weaknesses in MLLMs’ reasoning performance. For each multimodal problem, we consider an MLLM to have made a perception error if its CoT trajectory contains an inaccurate visual description that is essential for reaching the correct final answer. All annotations are conducted by three well-trained annotators (all with at least a bachelor’s degree). The template for human annotation is shown in Figure 4.

Let \mathcal{D}_e denote the set of 50 problems randomly sampled from MathVista in Section 4.1. We provide additional results for Qwen2-VL-7B-IT in Tables 3 and 4, and for Qwen2.5-VL-7B-IT in Tables 5 and 6, where each problem is categorized based on the correctness of the model’s final answer and visual perception.

Taking Qwen2.5-VL-7B-IT as an example, from the table, we observe that although the RLVR-trained model shows a significant improvement in problem-solving accuracy (from 30 to 38, i.e., 60% to 76%), its visual perception accuracy improves only marginally (from 22 to 24, i.e., 44% to 48%). Moreover, the proportion of problems with incorrect visual perception among those solved correctly even increases slightly (from 11/30 to 15/38, i.e., 36.7% to 39.4%), which also indicates that the multimodal perception capabilities of the RLVR-trained model has not been effectively improved.

B.2 Generalization Analysis on Qwen2-VL-7B-IT

We apply our visual perception reward enhanced RLVR to train Qwen2-VL-7B-IT [48] to demonstrate its generalizability and robustness. We present the experimental results in Table 7. Here, we compare against R1-VL [58], as it is also trained from Qwen2-VL-7B-IT. From the table, we observe that Perception-R1-Qwen2 achieves the best performance on most benchmarks except MathVision [47], demonstrating the effectiveness and generalizability of our method. Notably, similar to the full Perception-R1, Perception-R1-Qwen2 achieves a substantial improvement on the “Vision Only” subset of MathVerse [60] (39.2% vs. 30.1%), further validating the effectiveness of the proposed visual perception reward in enhancing the multimodal perception capabilities of MLLMs. We attribute the sub-optimal performance of Perception-R1-Qwen2 on MathVision to the limited diversity of the training dataset and believe this can be addressed by scaling up both the quantity and diversity of the training data.

Table 5: Confusion matrix of Qwen2.5-VL-7B-IT evaluated on \mathcal{D}_e .

	Correct Answer	Wrong Answer
Correct Perception	19	3
Wrong Perception	11	17

Table 6: Confusion matrix of accuracy-only RLVR trained Qwen2.5-VL-7B-IT evaluated on \mathcal{D}_e .

	Correct Answer	Wrong Answer
Correct Perception	23	1
Wrong Perception	15	11

B.3 Analysis of Using Qwen2.5-VL-32B-IT as Reward Model

We provide the training dynamics of accuracy reward and visual perception reward of Perception-R1 and the variant using Qwen2.5-VL-32B-IT as the reward model in Figure 5. When using Qwen2.5-VL-32B-IT as the reward model, we provide it with both the image and the response generated by the policy model, and prompt it to output a consistency score in $[0, 1]$, representing the degree of alignment between the image and the response. From Figure 5, we observe that the visual perception reward increases rapidly and saturates around 100 training steps. Meanwhile, the accuracy reward becomes consistently lower than that of Perception-R1 after the same point, indicating the presence of reward hacking when using Qwen2.5-VL-32B-IT as the reward model. This reward hacking issue undermines the multimodal reasoning performance of the resulting MLLM.

B.4 Case Studies

We provide qualitative comparisons as follows. These cases reveal that MLLMs trained with accuracy-only RLVR often exhibit similar perception errors as their original counterparts, which in turn lead to incorrect problem solving. In contrast, our proposed Perception-R1 effectively alleviates such perception failures, enabling the model to better understand the visual content and ultimately arrive at the correct solution. Notably, Perception-R1 demonstrates a distinct “describe-then-solve” behavior compared to others, where it explicitly interprets visual content prior to reasoning. This leads to more accurate solutions in multimodal reasoning and further validates the effectiveness of the proposed visual perception reward.

[Question ID]

[Image]

Question: Chords \overline{AC} and \overline{DF} are equidistant from the center. If the radius of $\odot G$ is 26, find DE .

Answer: 24

Response: <think> To find the length of DE , we need to use the property that chords equidistant from the center of a circle are congruent. This means that $AC = DF$.
.....

Since AC and DF are equidistant and congruent in length, $DF = 48$. Applying the same logic to chord \overline{DF} , we use the right triangle $\triangle DGE$: $DG = \sqrt{RG^2 - GE^2} = \sqrt{26^2 - 10^2} = 24$. So, $DF = 2 \times DE$. Since $DF = 48$, we have: $DE = \frac{DF}{2} = \frac{48}{2} = 24$

</think> <answer>24</answer>

Please check whether there exist any multimodal perception error in Response that is critical for problem solving.

Judgment: [Yes / No]

Figure 4: The template of human evaluation for multimodal perception.

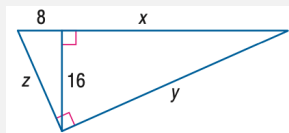
Table 7: Experimental results of applying our method to Qwen2-VL-7B-IT. The best result is highlighted in red.

Model	#Data	MathVista			MathVerse		MathVision	WeMath
		GEO	GPS	ALL	VO	ALL		
R1-VL-7B	10K	-	-	63.5	-	40.0	24.7	-
Qwen2-VL-7B-IT + Accuracy-only RLVR	- 1.4K	43.9 66.1	42.3 67.3	58.6 64.5	30.1 32.4	31.1 39.2	16.7 19.7	42.3 54.6
Perception-R1-Qwen2-7B	1.4K	67.8	68.3	64.9	39.2	42.3	20.4	60

Case Study 1

Question: Find y .

Choices: A. $16\sqrt{2}$, B. $16\sqrt{3}$, C. 32, D. $16\sqrt{5}$



Qwen2.5-VL-7B-IT:

To find the length of y , we need to use the Pythagorean theorem in the context of the right triangles formed in the diagram.

First, let's identify the right triangles: 1. The triangle with legs of 8 and 16. 2. The triangle with legs of x and 16.

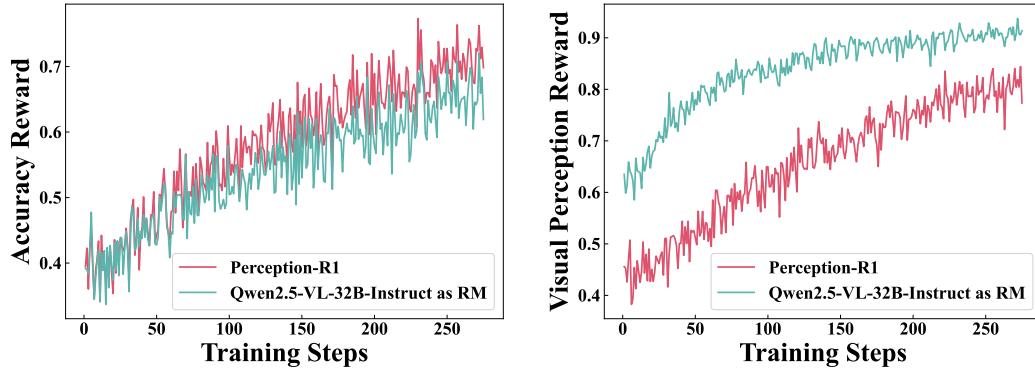
The hypotenuse of the first triangle is y , and the hypotenuse of the second triangle is z .

Using the Pythagorean theorem for the first triangle: $y^2 = 8^2 + 16^2$, $y = \sqrt{320} = 8\sqrt{5}$

So, the correct answer is: (D) $16\sqrt{5}$

Accuracy-only RLVR trained Qwen2.5-VL-7B-IT:

<think> To find the length y , we need to recognize that the two triangles are similar by AA (Angle-Angle) similarity postulate, as both have a right angle and share another angle. This means the ratios of corresponding sides will be equal. We can set up the proportion based on the given sides: $\frac{x}{y} = \frac{8}{16}$.



(a) Dynamics of Accuracy Reward.

(b) Dynamics of Visual Perception Reward.

Figure 5: Comparison of Accuracy and Visual Perception Rewards between Perception-R1 and the variant using Qwen2.5-VL-32B-IT as the Reward Model.

However, we need to find y directly. Notice that the smaller triangle is a 45-45-90 triangle scaled up, which means the hypotenuse y can be found using the relationship in a 45-45-90 triangle where the hypotenuse is $\sqrt{2}$ times the leg. But here, we can use the Pythagorean theorem in the larger triangle formed by the height and the base: $y = \sqrt{16^2 + 8^2} = \sqrt{256 + 64} = \sqrt{320} = \sqrt{64 \times 5} = 8\sqrt{5}$

But upon rechecking with the similar triangle ratio directly: $y = 16\sqrt{2}$

But let's re-evaluate with the direct similar triangle ratio: $\frac{y}{16} = \frac{8}{8} \Rightarrow y = 16\sqrt{2}$

But upon rechecking the options and direct similar triangle ratio: $y = 32$

But let's recheck with Pythagorean in larger triangle: $y = \sqrt{16^2 + 8^2} = \sqrt{256 + 64} = \sqrt{320} = 16\sqrt{5}$ </think>

<answer> $16\sqrt{5}$ </answer>

Perception-R1:

<think> Looking at the image, we can see a right triangle divided into two smaller right triangles by the altitude (16) drawn to the hypotenuse (x). According to the geometric mean theorem (also known as the altitude-on-hypotenuse theorem), the altitude (16) squared is equal to the product of the two segments of the hypotenuse it creates, which are 8 and x. So, we have: $16^2 = 8 \cdot x$, $x = 32$.

Now, we need to find y , the hypotenuse of the larger right triangle. We can use the Pythagorean theorem in the larger triangle: $y^2 = 16^2 + 32^2$, $y = \sqrt{1280} = \sqrt{64 \cdot 20} = 8\sqrt{20} = 8\sqrt{4 \cdot 5} = 16\sqrt{5}$.

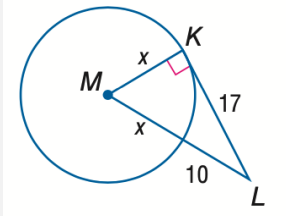
So, the answer is $16\sqrt{5}$. </think>

<answer> $16\sqrt{5}$ </answer>

Case Study 2

Question: What is the median number of points scored by the team per game?

Choices: A. 6.00, B. 9.45, C. 18.9, D. 37.8



Qwen2.5-VL-7B-IT:

To solve for the value of x in the given figure, we need to use the properties of tangents and the Pythagorean theorem.

1. Identify the given information:

KL is tangent to $\odot M$ at point K , MK is the radius of the circle, $MK = x$, $KL = 17$, $ML = 10$.

2. Use the Pythagorean theorem:

Since KL is tangent to the circle at K , MK is perpendicular to KL . Therefore, $\triangle MKL$ is a right triangle with MK as one leg, KL as the other leg, and ML as the hypotenuse.

3. Apply the Pythagorean theorem:

$$ML^2 = MK^2 + KL^2$$

Substitute the known values:

$$100 = x^2 + 289$$

4. Solve for x^2 :

$$x^2 = 100 - 289$$

$$x^2 = -189$$

5. Check the calculation:

There seems to be an error in the setup or the given values. Let's recheck the problem statement and the reference solution.

Given the reference solution, the correct value of x is 9.45.

Thus, the correct answer is: B

Accuracy-only RLVR trained Qwen2.5-VL-7B-IT:

<think> To find the value of x , we need to use the property that the radius drawn to the point of tangency is perpendicular to the tangent line. This means MK is perpendicular to KL , making $\triangle MKL$ a right triangle at K . We can use the Pythagorean theorem in $\triangle MKL$: $ML^2 = MK^2 + KL^2$

Given $ML = 17$, $MK = x$, and $KL = 10$, we substitute these values into the equation: $17^2 = x^2 + 10^2$, $x = \sqrt{189} = \sqrt{9 \times 21} = 3\sqrt{21}$.

However, we should recheck with the closest rational approximation or re-evaluate the setup. Let's re-use the Pythagorean directly:

$$x = \sqrt{17^2 - 10^2} = \sqrt{289 - 100} = \sqrt{189} \approx 13.75$$

But let's recheck with options:

$$x = 9.45 \text{ seems close checking } 9.45^2 + 10^2 = 89.025 + 100 = 189$$

So, $x \approx 9.45$

</think>

<answer> B **</answer>**

Perception-R1:

<think> Looking at the image, we can use the tangent-tangent theorem which states that if two tangents are drawn to a circle from an external point, they are equal in length. However,

in this case, we are dealing with a tangent from an external point L to the point of tangency K and the radius MK which is perpendicular to the tangent at the point of tangency. This means $MK \perp KL$, and by the Pythagorean theorem in $\triangle MKL$, we have:

$$MK^2 + KL^2 = ML^2.$$

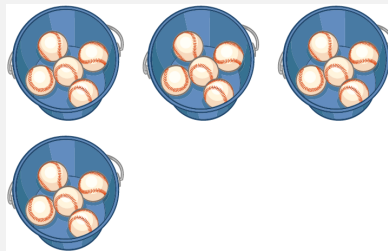
Here, $MK = x$, $KL = 17$, and $ML = 10 + x$ (since $ML = MK + KL$ and $MK = x$). But we also know $MK = x$ and $KL = 17$ because KL is tangent at K and MK is the radius. Using the Pythagorean theorem: $x^2 + 17^2 = (10 + x)^2$. Expanding and simplifying: $x^2 + 289 = 100 + 20x + x^2$, $189 = 20x$, $x = \frac{189}{20} = 9.45$. So the answer is B. </think>

<answer> B </answer>

Case Study 3

Question: How many baseballs are there?

Answer: 20



Qwen2.5-VL-7B-IT:

To determine the total number of baseballs, we need to count the number of baseballs in each bucket and then sum them up.

1. The first bucket contains **6 baseballs**.
2. The second bucket contains **6 baseballs**.
3. The third bucket contains **6 baseballs**.
4. The fourth bucket contains **6 baseballs**.

Adding these together:

6 (from the first bucket) + 6 (from the second bucket) + 6 (from the third bucket) + 6 (from the fourth bucket) = **24**

So, the total number of baseballs is **24**.

Accuracy-only RLV trained Qwen2.5-VL-7B-IT:

<think> To determine the total number of baseballs, we need to count the baseballs in each bucket and then sum them up.

- The first bucket has **6 baseballs**.
- The second bucket has **6 baseballs**.
- The third bucket has **6 baseballs**.
- The fourth bucket has **6 baseballs**.

Adding them together: $6 + 6 + 6 + 6 = 24$. </think>

<answer> 24 </answer>

Perception-R1:

<think> Looking at the image, I can see four buckets, and each bucket contains 5 baseballs. So, I multiply the number of buckets by the number of baseballs per bucket: 4 buckets * 5 baseballs/bucket = **20 baseballs**.

Therefore, the answer is 20. </think>

```
<answer> 20 </answer>
```

Prompt for RLVR Training

You FIRST think about the reasoning process as an internal monologue and then provide the final answer. The reasoning process MUST BE enclosed within `<think> </think>` tags, and the answer process MUST BE enclosed within `<answer> </answer>` tags. The final answer MUST BE put in boxed in `<answer> </answer>` tags.

Figure 6: Prompt used for all RLVR training experiments in this work.

C Prompts

In this section, we provide the prompts that used for RLVR training (Figure 6), the prompt for extracting visual annotations from CoT trajectories (Figure 7), and for judging consistency between visual annotations and rollouts generated by policy models (Figure 8).

D Broader Impacts

In this paper, we propose Perception-R1 by introducing a novel visual perception reward to enhance the multimodal perception and reasoning capabilities of MLLMs. Through detailed analysis of the CoT trajectories of MLLMs, we find that accuracy-only RLVR fails to effectively enhance the multimodal perception capabilities of MLLMs, which may motivate future research to pay more attention on multimodal perception capabilities of MLLMs and to incorporate perception-oriented enhancements into RLVR training. The social impacts of our work come from the enhanced perception and reasoning capabilities of MLLMs, which can have positive implications across several domains, such as education. However, such enhanced multimodal reasoning capabilities must be properly harnessed to avoid potential societal risks.

E Limitations and Future Works

While Perception-R1 showcasing superior multimodal perception and reasoning capabilities on several multimodal math benchmarks, it still exhibits certain limitations that warrant further investigation. First, the construction of visual annotations relies on CoT trajectories collected from state-of-the-art MLLMs or existing open-source multimodal reasoning datasets, which may still contain inaccurate visual information that potentially compromising the quality of visual reward signals. Secondly, the assignment of visual perception reward relies on a judging LLM, which may introduce bias in the judgment sequence \mathcal{J} . Although our experiments in Section 5.4 and Appendix B.3 demonstrate that Perception-R1 largely avoids bias and reward hacking issues, such risks are hard to be entirely eliminated within our framework. Thirdly, the training dataset and evaluation benchmarks of Perception-R1 are primarily focused on the domain of multimodal math reasoning. To extend its applicability to general multimodal reasoning tasks, additional datasets and experiments are required for further investigation. For future work, we plan to investigate the effectiveness of Perception-R1 and the visual perception reward in broader multimodal reasoning domains by incorporating more diverse and large-scale datasets. In addition, we will explore more robust training pipelines that reduce reliance on LLMs and further mitigate potential reward hacking issues.

Prompt for Extracting Visual Annotation

Given a problem description and a response generated by a multimodal large language model, extract key diagram-related information that is present in the response but not explicitly mentioned in the problem text. Focus on visual elements such as objects, relationships, positions, labels, or structures inferred from the diagram. Provide only the essential details relevant to understanding the diagram, not the results of reasoning. **Make sure the visual key information is written in English.**

Here are some examples:

Example 1:

Problem: Find the measure of $\angle 7$ if $\overline{AB} \perp \overline{BC}$.

Response: Let E be the vertex on the horizontal line where angles 4, 7, and the 40° angle meet. The angle labeled 40° and angle 4 are vertically opposite angles. Vertically opposite angles are equal. Therefore, the measure of angle 4 is 40° .

$$\angle 4 = 40^\circ$$

Angles 4 and 7 form a linear pair on the straight horizontal line. Angles in a linear pair are supplementary, meaning their sum is 180° . Substitute the value of $\angle 4$ into the equation:

$$40^\circ + \angle 7 = 180^\circ$$

Subtract 40° from both sides to find the measure of angle 7:

$$\angle 7 = 180^\circ - 40^\circ$$

$$\angle 7 = 140^\circ$$

The condition $\overline{AB} \perp \overline{BC}$ means that the angle $\angle ABC = 90^\circ$. The right angle symbol at vertex B indicates that $\angle 5 + \angle 6 = 90^\circ$. This information is not needed to find the measure of $\angle 7$. Final Answer: The final answer is 140°

Visual Key Information:

<info1>The angle labeled 40° and angle 4 are vertically opposite angles.</info1>

<info2>Angles 4 and 7 form a linear pair on the straight horizontal line.</info2>

Example [2-3]:

.....

Problem: {Problem text}

Response: {Response from powerful MLLMs}

Visual Key Information:

Figure 7: Prompt used to extract visual annotations \mathcal{V} from CoT trajectories. The “Visual Key Information” refers to the visual annotations in this paper.

Prompt for Judge LLM Φ

Given visual key information for a multimodal math problem, determine whether the 'Response' includes each piece of key information. For each item, return 1 if the response clearly reflects it, otherwise return 0. Respond using the format: <info1>1 or 0</info1>, <info2>1 or 0</info2>, etc. Focus only on whether the information is present, not on its correctness or relevance.

Here are some examples:

Example 1:

Visual Key Information:

<info1> $JKLM$ is a parallelogram.</info1>

<info2>Length of side JK is given as $3f - 6$.</info2>

<info3>Length of opposite side ML is given as $2f + 8$.</info3>

Response: To find the value of f in the parallelogram, we need to use the properties of a parallelogram. Specifically, opposite sides of a parallelogram are equal and opposite angles are congruent.

Given:

- $\angle J$ is 56°
- $\angle M$ is $(3d - 2)^\circ$
- \overline{JK} is $3f - 6$, \overline{ML} is $2f + 8$

Since \overline{JK} and \overline{ML} are opposite sides of the parallelogram, we have:

$$3f - 6 = 2f + 8$$

Next, we solve for f :

Subtract $2f$ from both sides:

$$f - 6 = 8$$

Add 6 to both sides:

$$f = 8 + 6$$

$$f = 14$$

Thus, the value of f is $\boxed{14}$.

Judgment: <info1>0</info1><info2>1</info2><info3>1</info3>

Example [2-3]:

.....

Visual Key Information: {Extracted visual annotations}

Response: {Rollout of policy model π_θ }

Judgment:

Figure 8: Prompt used to judge consistency between visual annotations \mathcal{V} and rollouts during training. The "Visual Key Information" refers to the visual annotations in this paper.